Journal of Achievements in Materials and Manufacturing Engineering
VOLUME 45
ISSUE 2
April
2011

A experiment study for welding optimization of fillet welded structure

H.H. Na [a,*], I.S. Kim [a], B.Y. Kang [b], J.Y. Shim [b]
[a] Department of Mechanical Engineering,
Mokpo National University, 534-729, South Korea
[b] Environmentally Materials & Components Center, KITECH, 561-202, South Korea
* Corresponding author: E-mail address: 1984octet@mokpo.ac.kr

Received 11.02.2011; published in revised form 01.04.2011

Analysis and modelling

ABSTRACT

Purpose: This study aims to examine the interaction between process parameters and bead geometry, to perform the research to predict optimal bead geometry (bead width, reinforcement height, left leg length, right leg length) through the analysis of experimental data. For this, not only linear and the curvilinear equations were developed to predict bead geometry, but also interactions between process parameters and bead geometry were analysed through sensitivity analysis.
Design/methodology/approach: A Taguchi method was applied for the optimization of process parameters, as well as bead geometry was predicted using a Neural Networks (LM) learning algorithm.
Findings: The data generated through experimental studies conducted in this study has employed to validate its effectiveness for the optimization of bead geometry on process parameters (welding current, welding voltage, welding speed), and to present the criteria to control the process parameters to achieve a good bead geometry.
Research limitations/implications: By applying Taguchi method, process parameters (welding current, welding voltage, welding speed) and bead geometry (bead width, reinforcement height, leg length) were analysed.
Originality/value: This study has developed mathematical models and algorithms to predict or control the bead geometry in GMA fillet welding process, and analysed the S/N ratio to which Taguchi theory was applied for sensibly to the process parameters.
Keywords: Taguchi method; Welding optimization; GMA

Reference to this paper should be given in the following way:
H.H. Na, I.S. Kim, B.Y. Kang, J.Y. Shim, A experiment study for welding optimization of fillet welded structure, Journal of Achievements in Materials and Manufacturing Engineering 45/2 (2011) 178-187.

1. Introduction

Today, GMA (Gas Metal Arc) welding is one of the most popular welding methods, especially in industrial environments due to the wide range of weldable metals, low in cost, high level of productivity and easy to learn. It is also popular in robot welding, in which robot handles the workpieces and the welding gun to quicken the manufacturing process.

The constructive machine defect on according the impacted load of workplace resulted in frequent failure of the important parts. The actual conditions occurring mainly from the welding procedures of each absence were necessary that solution for spatial-temporal process needs to be decided for constructive mechanical reliability. The necessary solutions for constructive mechanical welding crack are weldability characteristic security, various welding execution, conditional improvement and finally welding optimization research.

The GMA welding is a process that involves the melting and solidification of the joined materials. To make effective use of the robotic GMA welding process, it requires development of

mathematical models, which can be programmed easily and fed to the robot. It should give a high degree of confidence in predicting the bead shape to accomplish the desired mechanical properties of the weldment. In GMA welding, the process parameters are known to include welding current, welding voltage, welding speed, electrode extension, electrode orientation, weld joint position, wire diameter, shielding gas composition, gas flow rate, material composition and material thickness. Not only the process parameters are interdependent, but also the effect of one process parameter might affect another. In addition, interrelationships between process parameters and bead geometry are generally complex so that the required control system will be dependent on a realistic model of the welding process. The shape of bead geometry and occurrence of various weld defects such as incomplete penetration and undercut are also affected by all of these parameters [1].

Nagesh and Datta [2] applied the back-propagation neural network to predict the bead geometry in shielded metal-arc welding process. They claimed that the neural network is a workable model to predict the bead geometry and penetration under a given set of welding conditions. Also, Li et al. [3] modelled the non-linear relationship between the five geometric variables (bead height, bead width, penetration, fused and deposited areas) and process parameters (welding current, welding voltage and welding speed) of Submerged Arc Welding (SAW) process using the self-adaptive offset network.

Tarng et al. [4] predicted the welding parameters in laser butt welding using the back-propagation and Learning Vector Quantization (LVQ) neural network. They considered the input parameters of the neural network were to be workpiece thickness and welding gab, while the output parameters were to be the optimal focused position, acceptable welding parameters of laser power and welding speed.

Recently, not only robotic welders have replaced human welders in many welding applications, but also reasonable seam tracking systems are commercially available. However, fully adequate process control systems have not been developed due to a lack of reliable sensors and mathematical models that correlate welding parameters to the bead geometry for the automated welding process. Especially, real-time quality control in automated welding process is an important factor to higher productivity, lower costs and greater reliability of the bead geometry. Therefore, several researches have attempted to develop a monitoring and control technique for real-time welding quality [5-8]. Especially, many researchers know that a new algorithm to keep welding quality are important so they applied Artificial Intelligence (AI) methods such as neural network, to the development of predicted models in real-time techniques [9-11].

However, most previous studies of the analysis on butt-weld for prediction of bead geometry has been performed, but there is very limited literature describing the effects of process parameters on fillet welding. This study has developed mathematical models and algorithms to predict or control the bead geometry in GMA fillet welding process, and analyzed the S/N ratio to which Taguchi theory was applied for sensibly to the process parameters.

2. Experimental works

2.1. Design of experiment using Taguchi method

The experimental procedure included experimental design by Taguchi method, welding materials, welding equipment and welding procedure. Taguchi method can study data with minimum experimental runs. In this paper, the design of experiment work can be decided by this method. According to the experiment conditions in GMA welding process for fillet welding, the number of level settings and their levels by fillet welding for each process parameter is chosen to WPS and listed in Table 1. Based on Taguchi method, 23 (L9) orthogonal array with four columns and nine rows was employed. The assigned process parameters are listed in Table 2.

Each process parameter is assigned to a column and each row corresponds to one experimental run. For example, weld run No. 1 in the design matrix and the treatment combinations was made under the welding conditions coded as 1, 1, 1, which means that the welding current, welding voltage and welding speed were 240 A, 23 V and 40 cm/min respectively.

Table 1.
Process parameters and their levels for fillet welding

Parameters	Symbol	Level		
		Low	Middle	High
Welding Current (A)	I	240	260	280
Arc voltage (V)	V	23	25	27
Welding Speed (S)	S	40	45	50

Table 2.
Experimental Layout Using Orthogonal Array

No.	Welding Current (A)	Welding Voltage (V)	Welding speed (S)
1	1	1	1
2	1	2	2
3	1	3	3
4	2	1	2
5	2	2	3
6	2	3	1
7	3	1	3
8	3	2	1
9	3	3	2

2.2. Experimental procedure

The experimental procedure to measure bead geometry using input weld conditions was performed as following. In this experimental work, the CM-1 350A welding machine was employed shown in Fig. 1. In addition, the welding carriage and guide rail, wire feeder and fixed jig of welding specimen for the experimental configuration in shown in Fig. 1. The basic setting on the CM-1 350A welding machine was carried before welding

process. The experimental material 200×400×12, 20 mm steel S400 plates were fixed by the prepared jig. Tables 3-4 show mechanical properties and chemical composition of base metal and 100% CO_2 shielding gas which was employed in the experiment as shown in Fig. 2. The required input parameters were set through the welding machine manipulator by the use of program unit. The welding processes were started by turning on the welding machine and CO_2 shield gas.

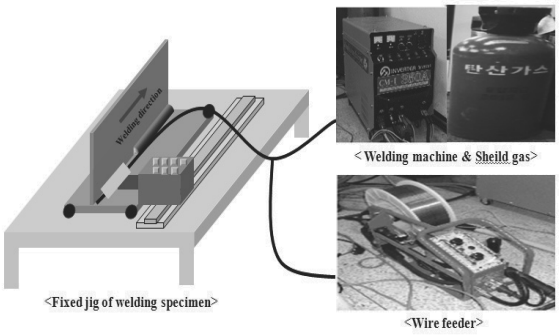

Fig. 1. Schematic diagram for experiment

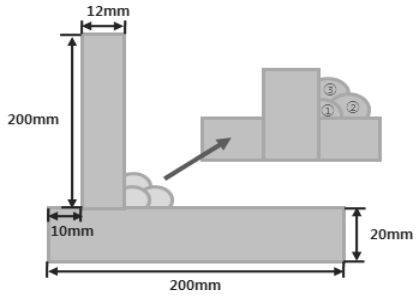

Fig. 2. Configuration of welding specimen

Table 3.
Mechanical properties of base metal

Base metal	Tensile Strength (kg/mm^2)	Yield Point (N/mm^2)	Elongation (%)	Impact Value (kgm/cm^2)	Hardness (Hv)
S400	43.5	32.5	25	6.2	128

Table 4.
Chemical composition of base metal

Material	Element (%) C	Mn	Cu	Cr	Ni	Fe
S400	0.15	0.69	0.04	0.08	0.50	Bal.

After the welding process, the material plates were removed from the jig and new plates were then fixed on the jig. In this way the eighteen experimental runs were carried out. To measure the bead geometry, the bead section was cut transversely from the middle position using the cutting machine. The incised plane was the specimen and then it was polished. In order to assure the precision of the specimen dimensions, it was etched by HNO_3 3% and H_2O 97%. The photos of the etched plates were taken by optical microscope and then the measurements of the bead geometry were obtained by the use of the Photoshop program.

To evaluate the quality of GMA welding, the measurements of the bead geometry were performed: bead width, reinforcement height, left leg length and right leg length. In this case, leg length is generated such as left leg length and right leg length. The fillet welding schematic diagram of bead geometry is shown in Fig. 3.

The experiment results of the GMA welding were obtained and were shown in Table 5.

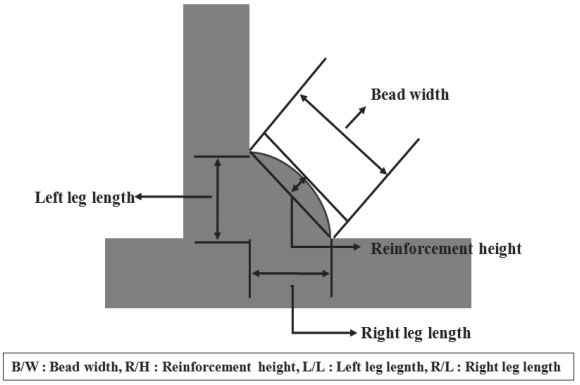

Fig. 3. A schematic diagram of bead geometry for the study

Table 5.
Experiment results of fillet welding

No.	Bead geometry	Bead width (mm)	Reinforcement Height (mm)	Left leg length (mm)	Right leg length (mm)
1	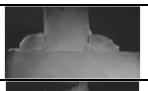	6.2	0.7	3.85	5.50
2		6.5	0.4	3.60	5.65
3		6.7	0.5	4.25	4.95
4	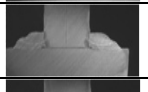	6.3	0.9	3.40	6.30
5	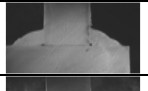	6.7	0.8	4.05	5.15
6		6.8	1.0	4.50	6.25
7		6.9	0.7	3.25	6.00
8	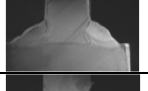	6.9	1.2	4.30	6.20
9	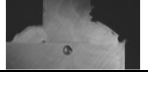	6.8	0.9	4.25	6.00

3. Experimental analysis and discussions

3.1. Development of empirical model

In this study, analysis of variance technique was used in the experimental design. Quantification of each bead parameters was examined through the significance of the variables for the optimal and analysis of the interaction between process parameters and optimal bead geometry. Adequacy of alignment was calculated by multiple correlation coefficient and Fisher's F-ratio. In addition, logical form of the equation by significance of Fisher's F-ratio 10% level was considered.

Using the experimental results obtained from the least squares regression, analysis based on bead geometry as a testament to the important action and reaction of Fisher's F-ratio from 1% significance level, the following equation can be calculated.

1) Bead width (B/W)

$$B/W = -19.30656 + 0.0367I + 2.456V - 0.83717S + 0.0002I^2 - 0.0208V^2 + 0.0067S^2 - 0.005IV + 0.0007IS + 0.0029VS \quad (1)$$

2) Reinforcement height (R/H)

$$R/H = -38.5589 + 0.2771I + 0.051233V + 0.02S - 0.0004I^2 - 0.0042V^2 + 0.0033S^2 - 0.0011IV - 0.0013IS - 0.0029VS \quad (2)$$

3) Left leg length (L/L)

$$L/L = 3695 + 0.125933I + 1.029803V - 1.71144S - 0.00017I^2 - 0.01667V^2 + 0.01133S^2 - 0.0018IV + 0.0003IS + 0.02VS \quad (3)$$

4) Right leg length (R/L)

$$R/L = -72.3131 + 0.3088I - 0.9869V + 2.37853S - 0.0005I^2 + 0.0417V^2 - 0.0123S^2 - 0.002IV - 0.0017IS - 0.04VS \quad (4)$$

Suitability of curvilinear equations is analysed by using analysis of variance. Multiple correlation coefficient of developed linear equation is 70% match, and it was found that bead width can be predicted. Table 6 shows that SSE, R Square and Adjusted R Square of linear equations developed.

Table 6.
Variance test of curvilinear model on bead geometry

No. eq	SSE	R Square	Adjusted R Square
(1)	0.87562	93.5%	74.1%
(2)	0.67243	88.7%	54.9%
(3)	0.97468	93.6%	74.4%
(4)	1.19594	79.4%	17.5%

Comparison between the predicted and measured bead geometry based on each linear equations is shown in Figs. 4-7. Most of the values converge within 10% margin of errors that could be confirmed.

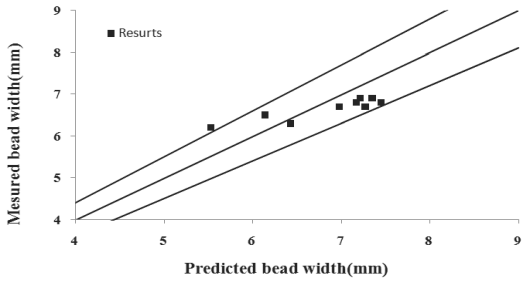

Fig. 4. Analysis of bead width on curvilinear model

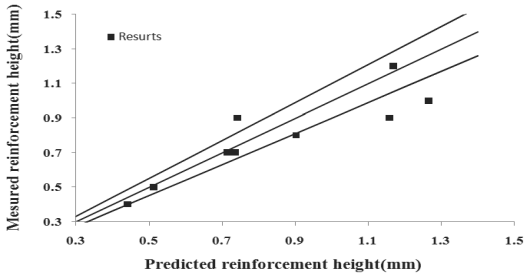

Fig. 5. Analysis of reinforcement height on curvilinear model

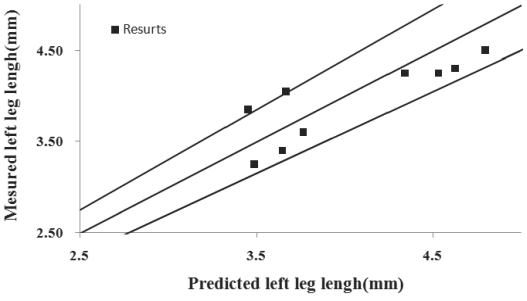

Fig. 6. Analysis of left leg length on curvilinear model

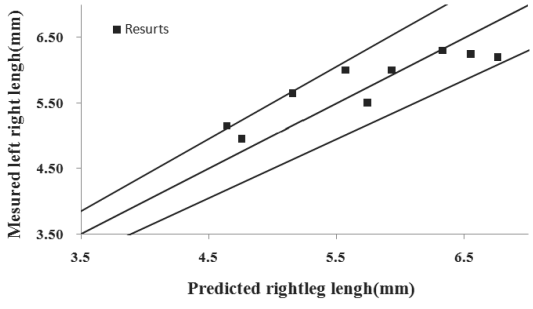

Fig. 7. Analysis of right leg length on curvilinear model

To determine the accuracy and efficiency of developed bead geometry, percentage deviation equation was employed, as follows:

$$\lambda = \frac{R_A - R_E}{R_E} \times 100 \quad (5)$$

Here, λ is percentage error, R_A calculation result, R_E experimental result. The percentage values of the equation, as shown in Fig. 8, were determined as six items: 0-5%, 5-10%, 10-15%, 15-20%, 20-25%, 25-30%. After analysis of bead geometry, most of models developed for GMA welding showed variation of less than 10%, making the correct bead size. To analyze the result of experiments, it was found that the calculated result can predict accurately the measuring values.

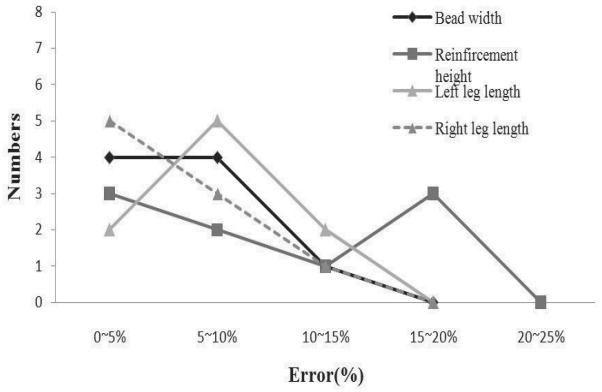

Fig. 8. Accuracy of the curvilinear model

3.2. Data analysis by a Taguchi method

To use the experimental results for the bead geometry using the L9 orthogonal array, bead penetration must basically be achieved to ensure the weld strength. According to Taguchi method, the actual equation for calculating the S/N ratio for the higher-the-better quality characteristic is a logarithmic function based on the mean square deviation. The S/N ratio can be expressed as:

$$\eta_{ij} = -10 \log y_{ij}^{\ 2} \tag{6}$$

The results of the loss function for the bead width are shown in Fig. 9. Similarly, the results of the loss function for the reinforcement height, left leg length and right leg length are respectively shown in Figs. 10-12.

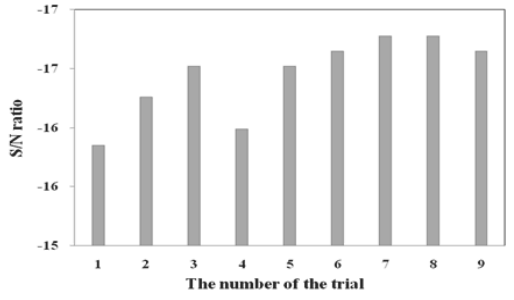

Fig. 9. S/N ratio of the bead width

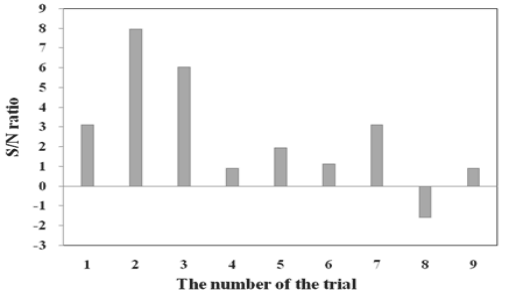

Fig. 10. S/N ratio of the reinforcement height

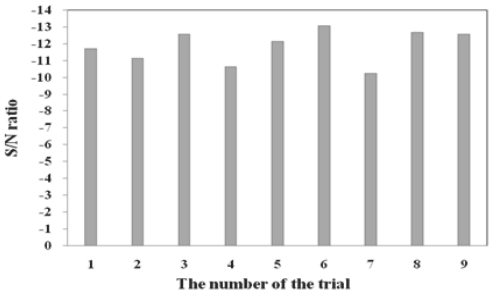

Fig. 11. S/N ratio of the left leg length

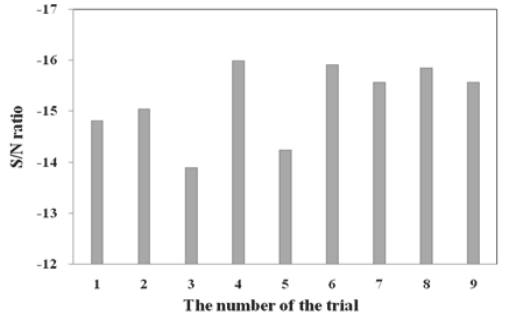

Fig. 12. S/N ratio of the right leg length

Using formulation (6) the quality characteristics corresponding to bead width, reinforcement height, left leg length and right leg length could be expressed in Figs 9-12. From Figs. 9-12, the largest values of the S/N ratios of the four quality characteristics are different. According to the Taguchi method, the larger is the S/N ratio, the better is the quality characteristic for the bead geometry. Therefore, the experiment 1, 2, 7, 3 for fillet multi-pass welding in Figs. 10-12 are the best ones based on the S/N ratios of the bead width, reinforcement height, left leg length and right leg length respectively. Therefore, it is difficult to decide the process parameters with the optimal bead geometry. Then another method was applied to consider the four quality characteristics together.

To consider the four quality characteristics together in the Taguchi method, a weighting method was employed to integrate the four loss functions into the overall loss function θ_j:

$$\theta_j = \sum_{i=1}^{k} \omega_i \eta_{ij} \tag{7}$$

where k is the number of the quality characteristics and ω_i is the weighting factor for the th quality characteristic. Here the weighting factors for the bead width and reinforcement height are selected as 0.1, while the weighting factors of the left leg length and right leg length are selected as 0.4. The S/N ratio corresponding to the overall loss function is shown in Fig. 13.

As shown in Fig. 13, the S/N ratio of experiment 2 for fillet multi-pass welding was the best multiple performance characteristic among the 9 experiments.

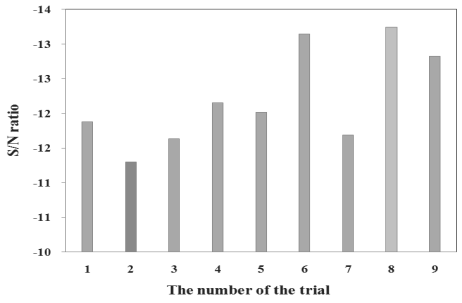

Fig. 13. S/N ratio of the bead geometry

Fig. 14 show the S/N ratio graph where the dashed line is the value of the total mean of the S/N ratio. Due to that, larger S/N ratio means better multiple quality characteristics for the bead geometry.

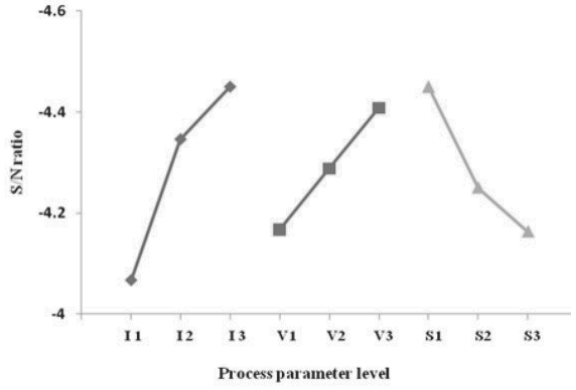

Fig. 14. S/N ratios for the bead geometry on process parameter

It can also be concluded from the Fig. 14 that the optimal level of the process parameter is I1, V1, S3. In other words, the case of optimal process parameters on fillet weld are welding current at level 1 and welding voltage at level 1 and welding speed at level 3. The S/N ratios of welding current and welding voltage vary greatly with the changes of the level. So among the process parameters, the welding current and welding voltage have a great effects on the bead geometry. The final step is to verify the experiment using the optimal level of the process parameters. So the optimal prediction of the bead geometry is included in the experiments which were already executed.

3.3. Sensitivity analysis of process parameters

To study the interactions between the process parameters (welding current, welding voltage, welding speed) and bead geometry, statistical method for multiple repression analysis was used. The multiple repression analysis has developed curvilinear equations such as formula ((1)~(4)) to predict bead geometry using a MINITAB, thecommercial statistical program and to investigate the interaction between process parameters and bead geometry as following:

$$B/W = -19.30656 + 0.0367I + 2.456V - 0.83717S + 0.0002I^2 - 0.0208V^2 + 0.0067S^2 - 0.005IV + 0.0007IS + 0.0029VS \quad (8)$$

$$R/H = -38.5589 + 0.2771I + 0.051233V + 0.02S - 0.0004I^2 - 0.0042V^2 + 0.0033S^2 - 0.0011IV - 0.0013IS - 0.0029VS \quad (9)$$

$$L/L = 3695 + 0.125933I + 1.029803V - 1.71144S - 0.00017I^2 - 0.01667V^2 + 0.01133S^2 - 0.0018IV + 0.0003IS + 0.02VS \quad (10)$$

$$R/L = -72.3131 + 0.3088I - 0.9869V + 2.37853S - 0.0005I^2 + 0.0417V^2 - 0.0123S^2 - 0.002IV - 0.0017IS - 0.04VS \quad (11)$$

On the basis of the curvilinear equation of bead geometry like the formulas (8-11) above, sensitivity equation can be obtained by differentiating the curvilinear equation by each process parameters (welding current, welding voltage, welding speed). The developed sensitivity equation was employed to evaluate the effects of each process parameters on the bead geometry. To assess the impact of each process parameter on the bead geometry, welding speed was fixed as 45 (cm/min), welding current was 240~260 (A), and welding voltage was changing in the range of 23 to 27 (V) to analyze the sensitivity on the bead geometry.

To obtain the sensitivity equation of bead width on the process parameters, equations (8-11) were respectively differentiated by each process variable. The equations (12-15) is a sensitivity equation of bead width, reinforcement height, left leg length and right leg length for welding current.

$$\partial W/\partial I = 0.367 - 0.0004I + 2.45V - 0.83647S + 0.0029VS - 0.0008V^2 + 0.0067S^2 \quad (12)$$

$$\partial H/\partial I = 0.2771 - 0.0008I + 0.052333V + 0.0187S - 0.0029VS - 0.0042V^2 + 0.0033S^2 \quad (13)$$

$$\partial L/\partial I = 0.125933 - 0.00034I + 1.028003V - 1.71114S + 0.02VS - 0.01667V^2 + 0.01133S^2 \quad (14)$$

$$\partial R/\partial I = 0.3088 - 0.001I - 0.9849V + 2.37683S - 0.04VS + 0.0417V^2 - 0.0123S^2 \quad (15)$$

The sensitivity equation for welding current can be determined by differentiating equations (8-11) by welding voltage. Such equation is shown as following;

$$\partial W/\partial V = 2.456 + 0.0317I - 0.416V - 0.83427S + 0.0007IS + 0.0002I^2 + 0.0067S^2 \quad (16)$$

$$\partial H/\partial V = 0.0512233 + 0.2782I - 0.0084V + 0.0171S - 0.0013IS - 0.0004I^2 + 0.0033S^2 \quad (17)$$

$$\partial L/\partial V = 1.029803 + 0.124133I - 0.0332V - 1.69144S + 0.0003IS - 0.00017I^2 + 0.01133S^2 \quad (18)$$

$$\partial R/\partial V = -0.9869 + 0.3108I + 0.0834V + 2.33853S - 0.0017IS - 0.0005I^2 - 0.0123S^2 \quad (19)$$

The sensitivity equation for welding speed can be determined by differentiating equations (8-11) by welding speed as shown in equations (20-23).

$$\partial W/\partial S = -0.83717 + 0.0374I + 2.4589V + 0.0134S - 0.005IV - 0.0208V^2 + 0.0002I^2 \quad (20)$$

$$\partial H/\partial S = 0.02 + 0.2758I + 0.048333V + 0.0066S - 0.0011IV - 0.0042V^2 - 0.0004I^2 \quad (21)$$

$$\partial L/\partial S = -1.71144 + 0.126233I + 1.049803V + 0.02266S - 0.0018IV - 0.01667V^2 - 0.00017I^2 \quad (22)$$

$$\partial R/\partial S = 2.37853 + 0.3071I - 1.0269V - 0.0246S + 0.002IV + 0.0417V^2 - 0.0005I^2 \quad (23)$$

The purpose of this investigation is to show the effects of process parameters by using sensitivity analysis on the curve equation developed. Tables 7-10 show the sensitivity of the calculated results for the selected process parameters such as bead width, bead height, penetration area, reinforcement area based on welding speed (S = 45 cm/min).

To consider the sensitivity of the calculated results as shown in Table 7, the sensitivity of welding current and welding speed is positive, where the sensitivity of welding voltage is negative. The sensitivity of the positive value indicates that as bead width increases, welding current or welding speed increases, and the sensitivity of the negative value indicates that as bead width decreases, welding voltage increases. We can see that as welding speed increases, the entire bead geometry including bead width is larger. Figs. 15-18 shows the sensitivity of process parameters (welding current, welding voltage, welding speed) on the bead geometry (bead width, reinforcement height, left leg length, and right leg length).

Table 7.
Sensitivities of process parameter on bead width

Welding Speed = 45 (cm/min)

Current (A)	Voltage (V)	$\partial W/\partial I$	$\partial W/\partial V$	$\partial W/\partial S$
240	23	24.43035	-4.39865	38.21333
	25	27.59655	-5.23065	38.73433
	27	30.59635	-6.06265	39.08893
260	23	24.43835	-1.13465	38.66133
	25	27.60455	-1.96665	38.98233
	27	30.60435	-2.79865	39.13693
280	23	24.44635	2.28935	39.26933
	25	27.61255	1.45735	39.39033
	27	30.61235	0.62535	39.34493

Table 8.
Sensitivities of process parameter on reinforcement height

Welding Speed = 45 (cm/min)

Current (A)	Voltage (V)	$\partial R/\partial I$	$\partial R/\partial V$	$\partial R/\partial S$
240	23	3.589459	36.99803	48.43086
	25	3.029925	36.98123	48.65233
	27	2.436791	36.96443	48.84019
260	23	3.573459	37.39203	50.45286
	25	3.013925	37.37523	50.71833
	27	2.420791	37.35843	50.95019
280	23	3.557459	37.46603	52.15486
	25	2.997925	37.44923	52.46433
	27	2.404791	37.43243	52.74019

Table 9.
Sensitivities of process parameter on left leg length

Welding Speed = 45 (cm/min)

Current (A)	Voltage (V)	$\partial L/\partial I$	$\partial L/\partial V$	$\partial L/\partial S$
240	23	-18.4881	-29.6654	25.20322
	25	-16.2324	-29.7318	24.83851
	27	-14.1101	-29.7982	24.34043
260	23	-18.4949	-28.6128	25.19988
	25	-16.2392	-28.6792	24.76317
	27	-14.1169	-28.7456	24.19309
280	23	-18.5017	-27.6961	25.06054
	25	-16.246	-27.7625	24.55183
	27	-14.1237	-27.8289	23.90975

Table 10.
Sensitivities of process parameter on right leg length

Welding Speed = 45 (cm/min)				
Current (A)	Voltage (V)	$\partial R / \partial I$	$\partial R / \partial V$	$\partial R / \partial S$
240	23	40.12525	108.6897	55.65613
	25	38.55865	108.8565	58.56553
	27	37.32565	109.0233	61.80853
260	23	40.10525	108.3757	57.71813
	125	38.53865	108.5425	60.70753
	27	37.30565	108.7093	64.03053
280	23	40.08525	107.6617	59.38013
	25	38.51865	107.8285	62.44953
	27	37.28565	107.9953	65.85253

From this, bead height and reinforcement height are mostly affected by the changes in welding speed. This is considered that an increase in the amount of deposition with the decrease of welding speed has to do with the increase in size of bead geometry. The left leg length and right leg length showed the highest sensitivity of welding speed and welding voltage, and the control of leg length can be effective to change the welding voltage and welding speed.

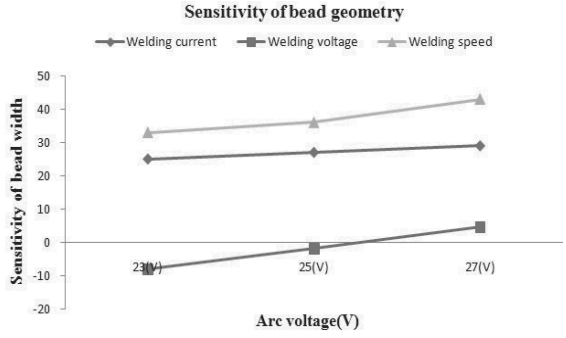

Fig. 15. Sensitivity analysis of bead width

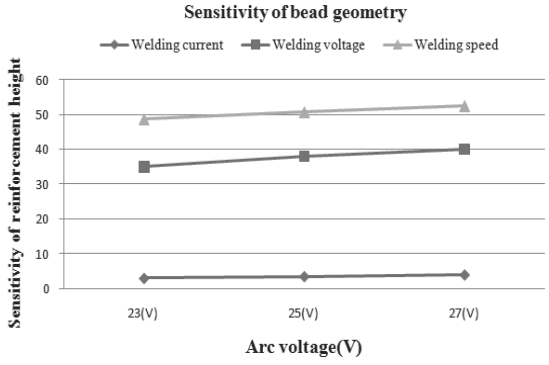

Fig. 16. Sensitivity analysis of reinforcement height

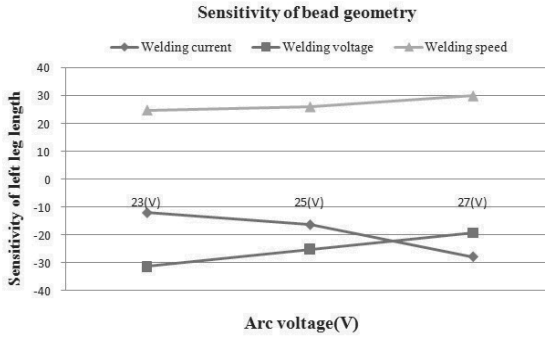

Fig. 17. Sensitivity analysis of left leg length

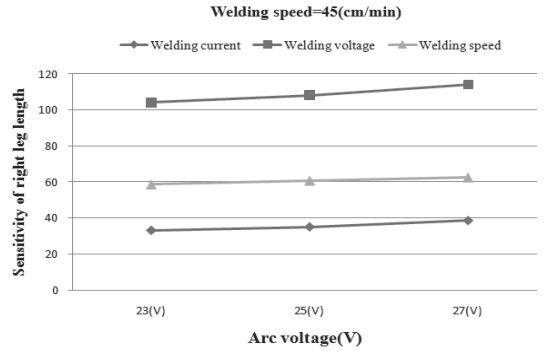

Fig. 18. Sensitivity analysis of right leg length

3.4. Prediction of optimal bead geometry using a neural network

To predict the bead geometry, LM neural network was employed. Levenberg-Marquardt algorithm was applied to predict bead geometry. Fig. 19 shows LM neural network used for predicting bead geometry. For the data used for each neural network learning, 108 data on 27 conditions obtained from experiments were used. In order to validate the learning neural network, additional experiments were conducted as shown in Table 11. And 8 data were obtained and neural network was verified using data acquired.

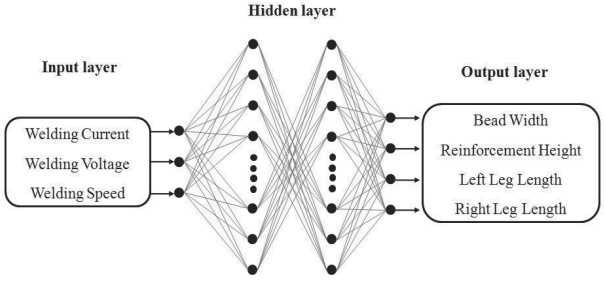

Fig. 19. LM neural network used for predicting bead geometry

Table 11.
Experiment results for verification of the neural network estimator

Trial No.	Welding current	Welding voltage	Welding speed	Bead width	Reinforcement height	Left leg length	Right leg length
1	240	23	40	6.25	0.74	3.85	5.54
2	240	25	45	6.54	0.64	3.62	5.65
3	240	27	50	6.73	0.58	4.25	4.95
4	260	23	45	6.34	0.92	3.44	6.36
5	260	25	50	6.79	0.86	4.05	5.15
6	260	27	40	6.81	0.87	4.53	6.25
7	280	23	50	6.95	0.76	3.25	6.58
8	280	25	40	6.94	1.04	4.38	6.29
9	280	27	45	6.86	0.98	4.25	6.78

Figs. 20-23 show the predicted results of bead width, reinforcement height, left leg length, right leg length on fillet welding process by using a neural network. As shown in the Figs. 20-23, it was confirmed that the boundary between measured and predicted values was within the range of tolerance 10% but, the error has been found to be relatively higher in the prediction range of bead width. The smaller the shape of bead is, the probability of error is higher. As shown in Fig. 24, LM neural network has higher reliability in the prediction of bead geometry on fillet welding.

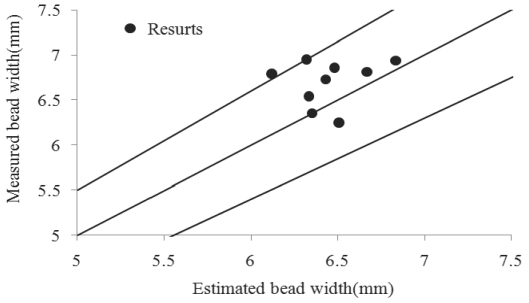

Fig. 20. Comparison of measured and predicted bead width using a neural network (LM)

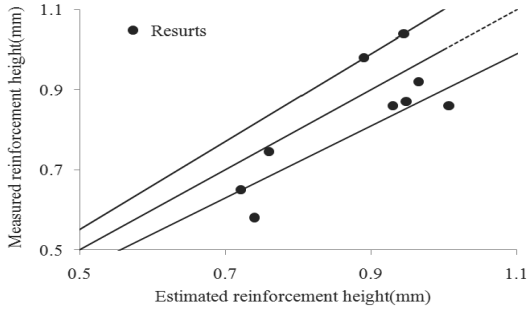

Fig. 21. Comparison of measured and predicted reinforcement height using a neural network (LM)

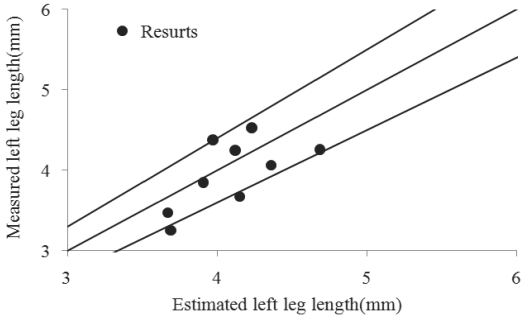

Fig. 22. Comparison of measured and predicted left leg length using a neural network (LM)

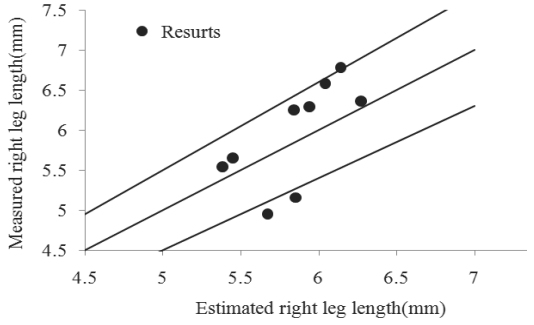

Fig. 23. Comparison of measured and predicted right leg length using a neural network (LM)

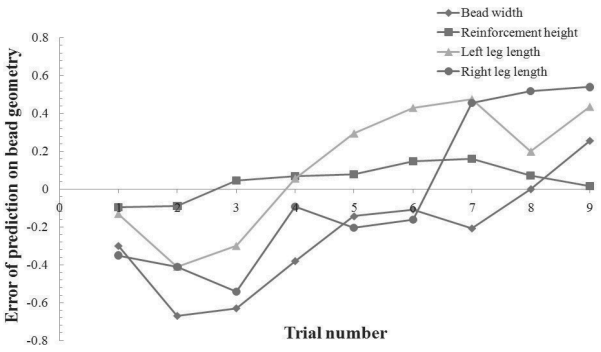

Fig. 24. Comparison of error in prediction for bead geometry using neural network (LM)

4. Conclusions

Based on the experimental results on fillet welding, regression analysis was developed linear and curve equations to predict bead geometry. The predicted values of the developed models showed distributions within 10% error range of experimental data. Also the authenticity of the equation developed has been verified for the prediction of bead geometry by comparing with the measure value. By applying Taguchi method, process parameters (welding

current, welding voltage, welding speed) and bead geometry(bead width, reinforcement height, leg length) were analyzed.

Through sensitivity analysis between process parameters and bead geometry, it has been found that bead geometry increased in its dimension depending on the welding current increased. The bead height and reinforcement height were sensitive to changes in welding speed. For the control of leg length, it is effective to change welding voltage and welding speed which is organically combined to affect bead geometry.

Bead geometry by applying learning and test data generated was predicted using LM neural network. As experimental result, the predicted values of bead geometry(bead width, reinforcement height, left leg length, right leg length) showed fairly accurate figures to the measured values. Setting the absolute value (predicted value minus actual measurement) as error, the performance of neural networks was analyzed. As a result, it showed that predicted values were distributed around measure values within the error range of less than 0.6 mm.

Acknowledgements

Following are results of a study on the "Human Resource Development Center for Economic Region Leading Industry" Project, supported by the Ministry of Education, Science & Technology (MEST) and the National Research Foundation of Korea (NRF).

References

[1] R.S. Chandel, S.R. Bala, Effect of welding parameters and groove angle on the soundness of root beads deposited by the SAW process. Advances in Welding Science and Technology, Proceedings of the International Conference “Trends in Welding Research”, Gatlinburg, Tennessee, USA, 1986, 479-385.

[2] D.S. Nagesh, G.L. Datta, Prediction of weld bead geometry and prediction in shielded metal-arc welding using artificial neural networks, Journal of Materials Process Technology 79 (2002) 1-10.

[3] P. Li, M.T.C. Fang, J. Lucas, Modelling of submerged arc welding bead using self-adaptive offset neural network, Journal of Materials Process Technology 71 (1997) 228-298.

[4] Y.S. Tang, H.L. Tsai, S.S. Yeh, Modelling, optimization and classification of weld quality in tungsten inert gas welding, International Journal of Machine Tools and Manufacturing 39 (1999) 1427-1438.

[5] Y.M. Zhang, R. Kovacevic, L. Li, Characterization and real-time measurement of geometrical appearance of the weld pool, International Journal of Machine Tools and Manufacture 36/7 (1996) 799-816.

[6] Y.W. Park, H.S. Park, S.H. Rhee, M.J. Kang, Real time estimation of CO_2 laser weld quality for automotive industry, Optics and Laser Technology 34/2 (2002) 135-142.

[7] J. Mirapeix, A. Cobo, O.M. Conde, C. Jauregui, J.M. Lopez-Higuera, Real-time arc welding defect detection technique by means of plasma spectrum optical analysis, NDT & E International 39/5 (2006) 356-360.

[8] C.H. Tsai, K.H. Hou, H.-T. Chuang, Fuzzy control of pulsed GTA welds by using real-time root bead image feedback, Journal of Materials Processing Technology 176/1-3 (2006) 158-167.

[9] M. Ushio, W. Mao, Dynamic Characteristics of Arc Sensor in GMA Welding in Dip Transfer Mode: A Study of the Improvement of the Sensitivity and the Reliability of Arc Sensor in GMA Welding (3rd Report), Journal of the Japan Welding Society 15/2 (1997) 272-280.

[10] S. Kodama, Y. Ichiyama, Y. Ikuno, N. Baba, Arc sensor sensitivity in short circuiting metal active gas welding with high speed torch oscillation, Science and Technology of Welding and Joining 11/1 (2006) 25-32.

[11] M. Guazzato, M. Albakry, Influence of Surface and Heat Treatments on the Flexural Strength of A Glass-infiltrated Alumina/Zirconia-reinforced Dental Ceramic, Dental Materials 21 (2005) 454-463.